Wireless Micro-ECoG Recording in Primates during Reach-to-Grasp Movements

Mohsen Mollazadeh, Elliot Greenwald and Nitish Thakor
Department of Biomedical Engineering
Johns Hopkins University
Baltimore, MD
Email: mohsenm@jhu.edu

Marc Schieber
Department of Neurology
University of Rochester Medical Center
Rochester, NY
Email: mhs@cvs.rochester.edu

Gert Cauwenberghs
Department of Bioengineering
University of California San Diego
San Diego, CA
Email: gert@ucsd.edu

***Abstract*— Electrocorticographic (ECoG) signals have emerged as a prominent neural interface signal modality due to their high bandwidth and availability in human subjects. We present a system for wireless recording of micro-ECoG activity in a primate performing reach-to-grasp movements. The system is comprised of a head-mounted interface, off-the-shelf receiver module, and custom software written in Labview for real-time data monitoring and storage. The head-mounted interface is composed of a custom-designed VLSI neural recording front, a commercially available FSK transmitter module, a digital interface, and a battery. The system offers a fixed gain of 40 dB, programmable bandwidth settings in the 0.1 Hz to 8.2 kHz range, digital gain of 1-16, and ADC resolution of 8-12 bits. The interface consumes 6.7 mA of current from a 3.7 V battery and transmits digitized data at 1 Mbps rate. The system offers less than 0.25% dropped packets at 3m non-line-of-sight distance. We then used the wirelessly recorded ECoG signal from the dorsal premotor cortex region to decode the movement state of the animal. The ECoG spectral features could decode the movement state, achieving close to 70% accuracy as early as 100 ms prior to actual movement onset. Our system offers a new avenue for future ECoG-based brain-machine interface systems.**

I. Introduction

There has been a tremendous effort towards designing head-mounted neural recording systems over the past few years. Two major goals motivate this drive: 1) recordings in awake behaving subjects to increase subjects interaction with the environment without interference from anesthesia effects or tethers and 2) the premise of using these systems in future brain-machine interfaces (BMI) [1] where subjects can directly interact with a device using their brain signals (e.g. control of a prosthetic device [2]). Several systems have been designed for recording spiking or local field potential (LFP) activity in awake subjects [3]–[9]. Szuts *et al.* [10] presented a system for wireless recording of spike or LFP activity in rodents in semi-natural environments.

Electrocorticography (ECoG), which measures the surface potentials from the cortex, is also emerging as prominent neural interface signal due to its high bandwidth and great stability. ECoG signals reflect the activity of large population of neurons under the recording electrode volume and have been proposed as a measure of synchrony between neuronal populations [11]. Moreover, it has been shown that ECoG signals contain information about arm motions [12], individual finger movements [13], and slow grasping motions [14]. Few systems have been developed for recording ECoG signals in primates. Zanos *et al.* [15] presented a system for wireless recording of ECoG and stimulation in freely moving monkeys.

We have previously presented a system for wireless recording of electroencephalography (EEG) activity in rodents [16] using a custom designed VLSI circuit [17]. Here, we present a system for wireless recording of micro-ECoG activity in primates performing reach-to-grasp movements. The system differs from our previous work in that it was directly integrated into the recording apparatus of an established experimental setup and included a different wireless module suitable for transmitting over long distances. Furthermore, we used the wirelessly recorded ECoG signals to decode the behavioral state of a primate during a motor task. The details of the system operation, performance of this system for BMI applications, and comparison to a commercial recording system are presented.

II. System Design

The functional block diagram of the system is shown in Fig. 1. The system incorporates a 16 channel VLSI neural interface, digital interface unit, wireless telemetry, and power supply unit. The neural data are amplified and digitized by the VLSI interface. The digital interface module receives the data from the chip, reformats and packages the data, and sends it to the telemetry module. Since only 8 ECoG channels were recorded, 8 channels of VLSI interface is shown in Fig. 1.

The neural interface circuit [17] contains 16 parallel differential voltage input, serial digital output channels for acquisition of neurophysiological signals. Each channel of the neural interface consists of a bandpass amplifier, a gm-C incremental $\Delta\Sigma$ ADC, and decimation and readout circuitry. Two stages of gain are implemented in the system: a constant gain in the front-end amplifier and a variable digital gain in the ADC stage. Tunable filtering is incorporated into the amplifier stage itself. The ADC offers programmable gain and resolution settings, allowing an optimal tradeoff between sampling rate and SNR. The digitized output then goes to the decimation and readout circuitry. The parallel-in serial-out circuitry of

978-1-4577-1470-2/11/$26.00 ©2011 IEEE

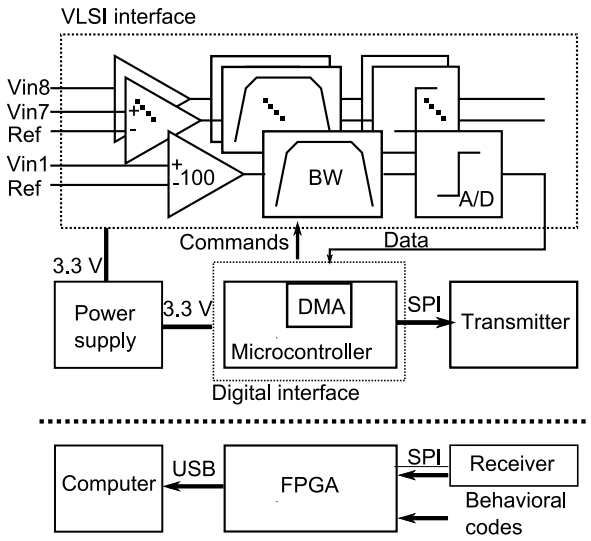

Fig. 1. Functional block diagram of the neural interface system. The dotted box shows the VLSI neural interface chip. The digitized neural output is sent to a commercial telemetry module through a microcontroller. Telemetered data is first read into an FPGA simultaneously with behavioral markers and then sent to a computer for real time display and storage.

each channel is connected in a daisy chain fashion to the next channel in order to have a single-bit serial output.

A microcontroller (PIC18F24J11 Microchip, Chandler, AZ) serves as the interface between the VLSI chip and the telemetry circuit (nRF24L01+ Nordic Semiconductor, Trondheim, Norway). The microcontroller provides the VLSI chip with required control settings including desired bandwidth, gain, and ADC resolution settings. Once a packet of data (96 bits at 256 Kbps) is received, the microcontroller sends the data to the telemetry module via its serial peripheral interface (SPI) at a 1Mbps rate (Fig. 3). This 96-bit packet consists of 8 channels of 12-bit ECoG data. The data transfer occurs using direct memory access (DMA) to avoid interrupting other operations. The microcontroller was operated at 1MHz instruction cycle to conserve power. Power was supplied to the system using a 3.7 V, 200 mAh rechargeable Li-Ion coin cell battery (Korea Power Cell, PD2450).

The telemetry circuit employed here can be configured as either a transmitter or receiver; the same model is therefore used on the receiving end. The transmitter module implements a cyclic-redundancy-check (CRC) in hardware and packets with bit-errors detected by the CRC are dropped automatically by the receiver. The received digitized data is read using an FPGA board (XEM3010 Opal Kelly, Portland, OR) controlled from LabView. The FPGA board also simultaneously accepts a DB-25 connector input which contains the markers for the behavioral events. These markers are generated by a central machine controlling the primate's experiment and can be written to all peripheral instruments. The behavioral data is interleaved with the neural data into a single FIFO and read into a computer using the USB port and displayed in real-time with custom software written in Labview. An arbiter, implemented in the FPGA, ensures that if neural data and behavioral data become available simultaneously, neither one can overwrite the other.

III. Animal Experiments

All animal experiments were approved by the University Committee on Animal Resources at the University of Rochester. Briefly, the monkey sits in a primate chair with its head restrained. Four objects, each evoking a different grasp pattern, were placed in a center out configuration in front of the monkey. The monkey was presented with a visual cue indicating which object to manipulate (Cue marker). After a random period, the monkey had to reach with his right arm (OM marker), grasp and manipulate the object (SWC marker). The monkey had to then hold the object for 1 sec to receive food rewards (RD marker). The sequence of behavioral events from a single trial is illustrated in Fig. 3. Details of the animal protocol for the experiments are described in [18]

The primate was implanted with multiple floating microelectrode arrays (Microprobe Inc., CA) in motor areas contralateral to the hand performing the movement. For the present report, we will only focus on one pseudo-ECoG array placed on dorsal premotor cortex (PMd). The array consists of 16 glass-insulated PtIr microelectrodes of different lengths, arranged in a 4x4 grid on a 4 mm^2 ceramic chip. For the present study, we will only focus on 8 electrodes with 0 mm length, i.e. the electrodes that record surface potentials only. In one recording session, we used the Plexon data acquisition system (Plexon Inc., Dallas, TX) with a gain of 1000 and hardware filtering of 0.7 Hz to 175 Hz at 1kHz sampling rate. In another recording session, we used the described wireless recording system (Fig. 2) with head-stage gain of 100 and filter range of 15 Hz to 500 Hz at 1 kHz sampling rate. The ADC full range was set to 2.5 mV_{pp}. The receiver circuitry was located approximately 3 m from the primate's chair.

IV. Feature Extraction and Decoding

All data analysis were performed in Matlab 2009b (Mathworks, Natick, MA). Spectral analysis was performed using multitaper method with 5 slepian tapers in 250 ms time windows with 50 ms time steps. A detailed description of the method can be found in [19]. The LFP power was then averaged in 4 frequency bands: 20-40 Hz, 40-60 Hz, 60-100 Hz, and 100-170 Hz. Our goal was to distinguish the movement onset from the baseline (-300 ms before the Cue). We then used linear discriminant analysis (LDA) to decode the behavioral state of the animal. The conditional probability $f_i(x)$ of belonging to class i was defined as,

$$f_i(x) \quad = \quad \mu_i C^{-1} x_k^T - \frac{1}{2}\mu_i C^{-1}\mu_i^T + ln(p_i) \qquad (1)$$

where x is the input feature set (ECoG power from all channels), C is the pooled within group covariance matrix, μ_i is the mean, and p_i is the prior estimate for the i^{th} group. The decoded output, $Y(t_k)$, was selected as the class with the highest conditional probability:

$$Y(t_k) \quad = \quad argmax_i \;\; f_i(x) \qquad (2)$$

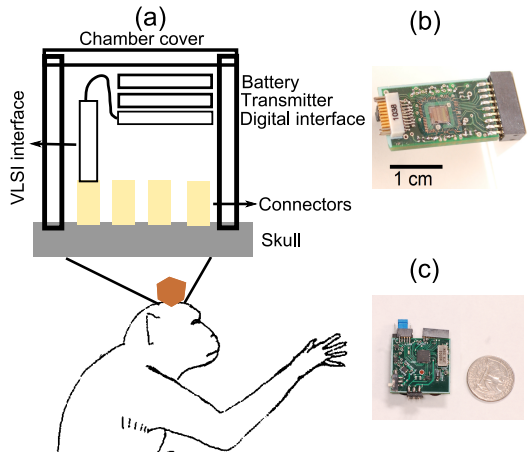

Fig. 2. (a) Cartoon drawing of the system assembly and placement on a monkey head. (b) Assembled VLSI neural interface board. (c) Assembled digital interface board.

Mutually exclusive feature sets were used for training and testing, and results were averaged using fivefold cross-validation. Separate decoding filters were built for ECoG power in each frequency band as well as the combination of all frequency bands.

V. Results

Fig. 2(a) shows a cartoon drawing of how the system was be assembled and placed on the primate's head. The VLSI interface chip (Fig. 2(b)) was wirebonded to a 1.1 in $\times$ 1.1 in printed circuit board (PCB) and directly connected to the omnetics connector (Omnetics Connector Corporation, MN) on primates head. The digital interface module, transmitter and battery were placed on a 1.3 in $\times$ 1.3 in PCB (Fig. 2(c)) and attached to the chambers cover. The two boards were connected using flexible custom-made cables. The whole system weighed 19 grams and could run continuously for more than 24 hours.

A. System Characterization

The VLSI chip was programmed for a 15 Hz to 500 Hz bandwidth, digital gain of 1, and ADC sampling rate of 1 kHz. Each channel had less than 0.1% total harmonic distortion and close to 54 dB signal to noise-distortion ratio. The whole system drew 6.7 mA of current from the battery and operated at 3 meters range in non-line-of-sight conditions. At this distance, the percent of dropped packets due to a CRC error in our recording session was 0.25%.

Fig. 3(a) shows the digital bitstream from the interface to the microcontroller at 256 kbps. Fig. 3(b) shows the digital packets sent from the microcontroller to the telemetry module at 1Mbps. The received data packet and simultaneous neural data are shown in Fig. 3(c)-(d) respectively. There was less than a millisecond delay between behavioral data received into FPGA and those read by the Plexon system.

B. In-vivo Results

Fig. 4 show the spectogram of wireless recorded neural activity from one channel averaged across all the successful

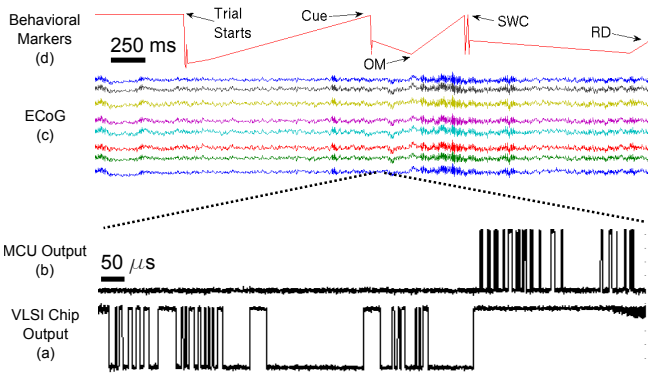

Fig. 3. (a) Digitized data is sent from VLSI interface to microcontroller at 256 kbps. (b) Data is reformatted and sent to the telemetry module at 1Mbps. (c) Received data is simultaneously read with (d) the behavioral data.

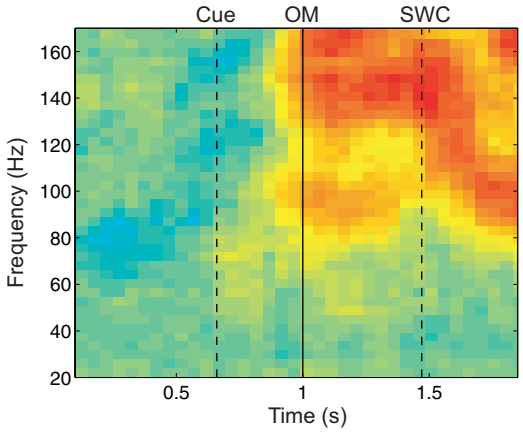

Fig. 4. Time-frequency spectrum of one wirelessly recorded ECoG channel. Data were aligned to onset of movement time (OM, solid vertical line). average cue presentation and switch closure times are presented with dashed vertical lines. Changes in high gamma power are evident around the movement onset time.

trials. Data were aligned to OM marker (solid vertical line). The dashed vertical lines show the average cue presentation and switch closure times. In general, most channels showed an increase in ECoG power in frequencies above 60 Hz (high gamma) around the onset of movement time.

As described before, we used the ECoG power features in the 15-22 Hz, 25-40 Hz, 40-60 Hz, 60-100 Hz, and 100-170 Hz to determine which state of the movement (baseline, or movement) the animal was in. Fig. 5(a) shows the classification accuracy results for each frequency band of the wireless and wired sessions at the movement onset time. As it can be seen, the ECoG power in the both 40-60 Hz and 100-170 Hz bands performed best among all frequency bands, similarly in both recording sessions. Using all spectral features slightly increased the decoding power.

Fig. 5(b) shows the state decoding accuracy over time using all the spectral features. As it can be seen, the spectral features could not distinguish the movement state from chance level (dashed horizontal time) till the cue presentation time as expected. However, even 100 ms before the onset of movement time, the ECoG spectral features in PMd area can decode

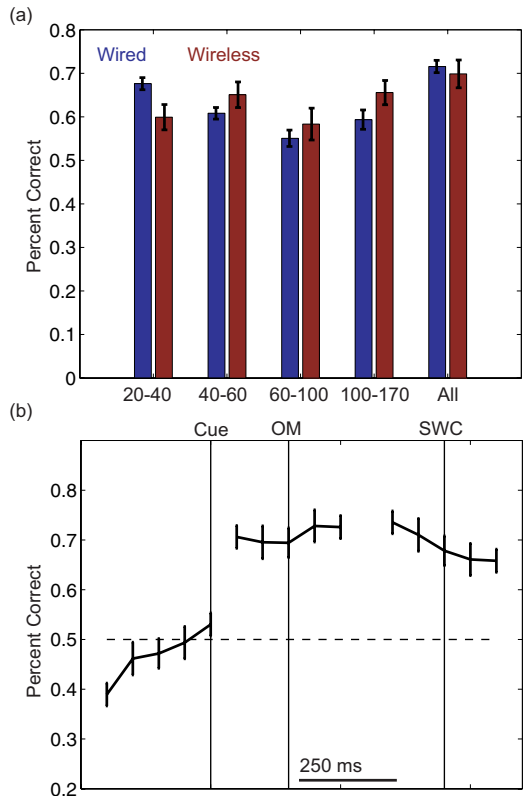

Fig. 5. (a) Decoding accuracy at the time of movement onset for each frequency band (b) Movement state decoding accuracy over time. ECoG features could decode movement state even 100ms prior to actual movement.

the movement onset. The decoding accuracy slowly decreases after the switch closure time.

VI. Conclusion

We have developed and tested a system for wireless recording of ECoG activity in an awake-behaving non-human primate. The system was based on a custom VLSI circuit with configurable gain, bandwidth, and ADC resolution settings suitable for all neural signal modalities [17]. Our system was then used to wirelessly record neural activity from the PMd area as the monkey performed reach-to-grasp movements. Similar to prior work where LFP activity from the parietal cortex [20] was shown to decode the onset of movement (or the "go" signal), we demonstrated that spectral ECoG features could also successfully decode the movement state. Our system have implications for future BMI systems where micro-ECoG signals can be acquired wirelessly and used to decode more complex movements in freely moving subjects.

Acknowledgment

The authors would like to thank Jay Uppalapati for help with the experiments, Kartikeya Murari for help with the system design and Matt Fifer for editorial comments. Chips were fabricated through the MOSIS foundry service. This work was supported by the DARPA REPAIR program, contract 19GM-1088724, and NIBIB R01-EB010100 grants.

References

[1] G. Dornhege, J. del R. Millan, T. Hinterberger, D. J. McFarland, and K.-R. Muller, *Towards Brain-Computer Interfacing*. Cambridge, MA, USA: MIT Press, 2007.

[2] L. R. Hochberg, M. D. Serruya, G. M. Friehs, J. A. Mukand, M. Saleh, A. H. Caplan, A. Branner, D. Chen, R. D. Penn, and J. P. Donoghue, "Neuronal ensemble control of prosthetic devices by a human with tetraplegia," *Nature*, vol. 442, no. 13, pp. 164–171, 2006.

[3] J. Mavoori, A. Jackson, C. Diorio, and E. Fetz, "An autonomous implantable computer for neural recording and stimulation in unrestrained primates," *J. Neurosci. Methods*, vol. 148, no. 1, pp. 71 – 77, 2005.

[4] A. L. Vyssotski, A. N. Serkov, P. M. Itskov, G. Dell'Omo, A. V. Latanov, D. P. Wolfer, and H.-P. Lipp, "Miniature neurologgers for flying pigeons: Multichannel EEG and action and field potentials in combination with GPS recording," *J Neurophysiol*, vol. 95, no. 2, pp. 1263–1273, 2006.

[5] G. Santhanam, M. Linderman, V. Gilja, A. Afshar, S. Ryu, T. Meng, and K. Shenoy, "HermesB: A continuous neural recording system for freely behaving primates," *IEEE Trans. Biomed. Eng.*, vol. 54, no. 11, pp. 2037–2050, Nov 2007.

[6] D. Lapray, J. Bergeler, E. Dupont, O. Thews, and H. Luhmann, "A novel miniature telemetric system for recording EEG activity in freely moving rats," *J. Neurosci. Methods*, vol. 168, no. 1, pp. 119–126, Feb 2008.

[7] R. Hampson, V. Collins, and S. Deadwyler, "A wireless recording system that utilizes Bluetooth technology to transmit neural activity in freely moving animals," *J. Neurosci. Methods*, vol. 182, no. 2, pp. 195–204, Sep 2009.

[8] R. Harrison, R. Kier, A. Leonardo, H. Fotowat, R. Chan, and F. Gabbiani, "A wireless neural/EMG telemetry system for freely moving insects," in *IEEE Int. Symp. Circ. Sys. (ISCAS'2010)*, May 2010, pp. 2940–2943.

[9] C. Chestek, V. Gilja, P. Nuyujukian, R. Kier, F. Solzbacher, S. Ryu, R. Harrison, and K. Shenoy, "HermesC: Low-power wireless neural recording system for freely moving primates," *IEEE Trans. Neural Sys. Rehab. Eng.*, vol. 17, no. 4, pp. 330–338, Aug 2009.

[10] T. Szuts, V. Fadeyev, S. Kachiguine, A. Sher, M. Grivich, M. Agrochão, P. Hottowy, W. Dabrowski, E. Lubenov, A. Siapas, *et al.*, "A wireless multi-channel neural amplifier for freely moving animals," *Nature Neuroscience*, 2011.

[11] S. Ray, N. E. Crone, E. Niebur, P. J. Franaszczuk, and S. S. Hsiao, "Neural correlates of high-gamma oscillations (60200 hz) in macaque local field potentials and their potential implications in electrocorticography," *The Journal of Neuroscience*, vol. 28, no. 45, pp. 11 526–11 536, 2008.

[12] Z. C. Chao, Y. Nagasaka, and N. Fujii, "Long-term asynchronous decoding of arm motion using electrocorticographic signals in monkey," *Frontiers in Neuroengineering*, vol. 3, 2010.

[13] J. Kubanek, K. Miller, J. Ojemann, J. Wolpaw, and G. Schalk, "Decoding flexion of individual fingers using electrocorticographic signals in humans," *J. Neural Eng.*, vol. 6, p. 066001, 2009.

[14] S. Acharya, M. Fifer, H. Benz, N. Crone, and N. Thakor, "Electrocorticographic amplitude predicts finger positions during slow grasping motions of the hand," *J. Neural Eng.*, vol. 7, p. 046002, 2010.

[15] S. Zanos, A. Richardson, L. Shupe, F. Miles, and E. Fetz, "The neurochip-2: an autonomous head-fixed computer for recording and stimulating in freely behaving monkeys," *IEEE Trans. Neural Sys. Rehab. Eng.*, 2011.

[16] E. Greenwald, M. Mollazadeh, C. Hu, W. Tang, E. Culurciello, and V. Thakor, "A vlsi neural monitoring system with ultra-wideband telemetry for awake behaving subjects," *IEEE Trans. Biomed. Circ. Sys.*, vol. 5, no. 2, pp. 112 –119, April 2011.

[17] M. Mollazadeh, K. Murari, G. Cauwenberghs, and N. Thakor, "Micropower CMOS integrated low-noise amplification, filtering, and digitization of multimodal neuropotentials," *IEEE Trans. Biomed. Circ. Sys.*, vol. 3, no. 1, pp. 1–10, Feb 2009.

[18] V. Aggarwal, M. Kerr, A. Davidson, R. Davoodi, G. Loeb, M. Schieber, and N. Thakor, "Cortical control of reach and grasp kinematics in a virtual environment using musculoskeletal modeling software," in *Conf Proc IEEE Eng Med Biol Soc Neural Eng*, 2011, pp. 388–391.

[19] P. Mitra and B. Pesaran, "Analysis of dynamic brain imaging data," *Biophysical Journal*, vol. 76, no. 2, pp. 691 – 708, 1999.

[20] H. Scherberger, M. R. Jarvis, and R. A. Andersen, "Cortical local field potential encodes movement intentions in the posterior parietal cortex," *Neuron*, vol. 46, no. 2, pp. 347 – 354, 2005.